Low-Frequency Sound Absorption of Organic Hybrid Comprised of Chlorinated Polyethylene and *N,N′*-dicyclohexyl-2-benzothiazolyl Sulfenamide

Shuichi Akasaka, Taiki Tobusawa, Yoichi Tominaga, Shigeo Asai, Masao Sumita

Department of Chemistry and Materials Science, Tokyo Institute of Technology, 2-12-1-S8-38, Ookayama, Meguro-ku, Tokyo 152-8550, Japan

Received 14 September 2004; accepted 19 April 2005
DOI 10.1002/app.22839
Published online 27 December 2005 in Wiley InterScience (www.interscience.wiley.com).

ABSTRACT: We investigated the sound absorption characteristics of an organic hybrid material comprised of chlorinated polyethylene (CPE) as the matrix polymer and *N,N′*-dicyclohexyl-2-benzothiazolyl sulfenamide (DBS) as the second component of an organic low-molecular-weight compound. We found specific crystallites, obtained by annealing, that generated new absorption for a low-frequency sound in a CPE/DBS blend. We observed two sound absorption peaks, around 300 and 1000 Hz, in the annealed CPE/DBS (50 : 50 w/w) blends, whereas those peaks were not observed in the untreated sample. There were two kinds of crystals with different melting points in the annealed samples. It was confirmed that the crystals with the lower melting point brought about sound absorption at a low frequency. The crystals that had the lower melting point were smaller and/or more disordered than the crystals that had the higher melting point. We calculated the fraction of these two types of crystals from differential scanning calorimetry and wide-angle X-ray diffraction measurements. The annealing or reannealing temperature specified the fraction of the crystal with the lower melting point, and the obtained crystal fraction characterized sound absorption frequency. Therefore, it is possible to control the sound absorption frequency of an organic hybrid by heat treatment such as annealing. © 2005 Wiley Periodicals, Inc. J Appl Polym Sci 99: 2878–2884, 2006

Key words: annealing; blends; morphology; WAXS; differential scanning calorimetry (DSC)

INTRODUCTION

Many recent studies have investigated on organic hybrid materials comprised of polymer matrices and fillers of organic low-molecular-weight compounds. The viscoelastic properties of organic hybrid materials composed of rubbery amorphous polymers and vitrified organic low-molecular-weight compounds, such as optimal combinations of chlorinated polyethylene (CPE), acrylic rubber, *N,N′*-dicyclohexyl-2-benzothiazolyl sulfenamide (DBS) and hindered phenol compounds have been extensively investigated. In every experimental system, a high damping performance was observed.[1–3] The obtained results verified the vibration damping of an organic low-molecular-weight compound accompanying interactions, such as hydrogen bonding. In the organic hybrid material comprised of CPE and hindered phenol compounds, there were further investigations of the chemical structure of the organic low-molecular-weight compounds,[4] of the degree of chlorination or the molecular weight of the CPE matrix,[5] and also of the addition of chlorinated paraffin,[6] which involved viscoelastic analysis. The effect of crystallization on viscoelastic properties[7,8] and the crystal structure of the organic low-molecular-weight compound also were studied.[9] Moreover, shape memory, self-adhesiveness, and self-restoration were reported for the organic hybrid material comprised CPE and AO-80, one of the hindered phenol compounds.[10] The coexisting of organic low-molecular-weight compounds and a polymer matrix seems to come about specific vibration phenomena. We identified a new phenomenon related to sound absorption, in the low-frequency region, in particular, in an organic hybrid material. We considered the application of this organic hybrid as a novel sound absorber in low-frequency bands.

There are three types of sound absorbers: the porous, resonator, and panel/membrane types. Porous-type material, such as polyurethane foam or glass wool, absorbs acoustic energy by air viscosity in pores—sound comes into porous material and vibrates air in the pores. This type material has shown

Correspondence to: M. Sumita (msumita@o.cc.titech.ac.jp).
Contract grant sponsor: 21st Century COE program "Creation of Molecular Diversity and Development of Functionalities," Tokyo Institute of Technology.
Contract grant sponsor: Japan Society for the Promotion of Science; contract grant number: 16206066.
Contract grant sponsor: Eno Scientific Foundation.

sufficient sound absorption above 500 Hz but insufficient absorption below 500 Hz. It is known that an absorbable frequency range expands to a lower frequency with increasing thickness of this type of absorber. Polyurethane foam, for example, requires the thickness to be from several tens of millimeters to several hundred millimeters in order to absorb below 500 Hz of sound vibration.[11] A resonator-type absorber is a structure comprising a perforated panel and a backside air layer. Holes of the panel as a mass and the backside air layer as a spring form a resonance system on the principle of the Helmholtz resonator. When sound with a resonance frequency—determined by a perforation rate, the thickness of the backside air layer, and the thickness of the panel—incident to this structure, air around the hole vibrates violently, and the acoustic energy is absorbed by the friction with the panel around the hole. This type of structure shows a peak near the resonant frequency in sound absorption coefficient measurement. Therefore, it can absorb low-frequency sounds, whereas an absorbable frequency range is narrow because of the peak profile and requires a thicker backside air layer to absorb low-frequency sound. The panel/membrane type absorber also, as with a resonator-type absorber, causes sound absorption by resonance, not by viscoelasticity of the panel or membrane. In this type of absorber, the panel/membrane and the backside air layer act as a mass and a spring, respectively. This type of sound absorber, therefore, shows a narrow sound absorption frequency range and requires sufficient thickness of the backside air layer to absorb low-frequency sounds. Presently, a combination of these types of sound absorbers is used to obtain effective sound absorption in a particular frequency range and performance. A thin sound absorption material for low frequencies, below 500 Hz, would be very useful as a sound-absorbing component.

Some organic low-molecular-weight compounds crystallized from a solution exhibit several melting points because of the formation of crystals of varying thermal stability, known as polymorphism. The crystallization behavior of polymorphs is complicated by the simultaneous occurrence of nucleation and crystal growth and transformation from a metastable form to a stable form. There have been some reports on the dependence of the operating factor, such as temperature[12] and solvent.[13] The crystallization behavior of the organic hybrid also is complicated. It is necessary for there to be not only nucleation and a crystal growth process but also a dispersion state in an amorphous polymer matrix and a process of aggregation of molecules restricted by interaction with the polymer matrix. These processes are strongly affected by thermal histories such as heating rate, cooling rate, and additional heat treatments. As mentioned above, the proposed novel sound absorber is composed of CPE/DBS systems, which are the result of the complexity of molecular dynamics.

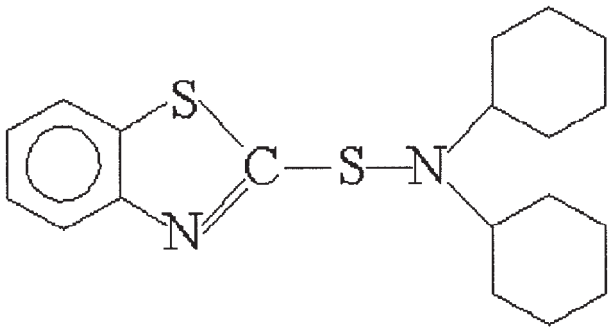

Figure 1 Chemical Structure of DBS.

In this study, we investigated the sound absorption of annealed CPE/DBS with reference to the crystalline fine structure of DBS.

EXPERIMENTAL

CPE with a degree of chlorination of 30 wt % (Elaslene 301A, Showa Denko K.K., Tokyo, Japan) was used as the matrix polymer, and DBS (shown in Fig. 1; Nocceler DZ, Ouchishinko Chemical Industrial Co., Ltd., Tokyo, Japan) was used as the organic low-molecular-weight compound. The melting point of the neat DBS crystal was about 103°C. DBS normally is used as an accelerator in sulfur vulcanization, but it is essentially effective below 190°C. The material was kneaded with a two-roll mill at 60°C. Then the mixture was melt-pressed at 140°C for 10 min under a pressure of 19.6 MPa, followed by quenching in ice water in order to obtain an amorphous film with a thickness of about 1 mm. Annealing and reannealing treatments were carried out at various temperatures in a vacuum.

The normal incident sound absorption coefficient (α) was measured with a sound absorption coefficient measurement system (Brüel & Kjær division, Spectris Co., Ltd., Tokyo, Japan) in a frequency range from 50 to 1600 Hz at room temperature. The measurement system was based on ISO 10534-2 : 1998, "Acoustics—Determination of sound absorption coefficient and impedance in impedance tubes—Part 2: Transfer-function method," or ASTM E 1050-90, "Standard test method for impedance and absorption of acoustical materials using a tube, two microphones, and a digital frequency analysis system." Figure 2 shows the schematic diagram of an impedance tube. It is composed of a speaker, two microphones, and a rigid movable wall. The space between a sample and the movable wall is called the backside air layer, and its thickness, *h,* is controlled by shifting the movable wall. The sample for this measurement was 100 mm in diameter and 1 mm thick. The sound absorption coefficient is the ratio

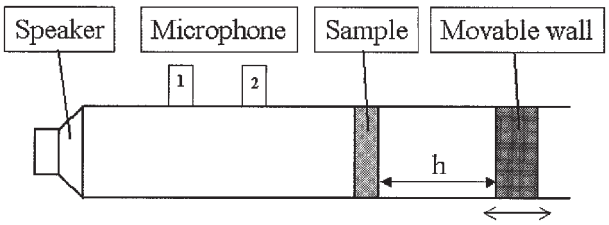

Figure 2 Schematic diagram of an impedance tube composing a normal incidence sound absorption coefficient measuring system.

of the intensity of an absorbed sound by a sample to that of an incident sound, and it is represented by the following equation:

$$\alpha = \frac{I_a}{I_i} = \frac{I_i - I_r}{I_i} \quad (1)$$

where I_a, I_i, and I_r are the intensities of the absorbed sound, the incident sound, and the reflected sound, respectively.

Differential scanning calorimetry (DSC) curves were obtained with a DSC8230 (RIGAKU Co., Tokyo, Japan) at a heating rate of 5°C/min under a nitrogen atmosphere. Each sample weighed about 5 mg. To calculate the crystallinity of DBS, we used 73.9 J/g as the enthalpy of fusion (ΔH_m) of the neat DBS crystal.

Wide-angle X-ray diffraction (WAXD) measurements were carried out with a RU200 (RIGAKU Co., Tokyo, Japan) operated at 50 kV and 180 mA using Cu Kα radiation with a wavelength of 1.5418 A. The WAXD patterns were recorded on an imaging plate (IP) by exposure for 30 min. The one-dimensional intensity profiles were obtained by the average in the azimuth range from 0 to 180°.

RESULTS AND DISCUSSION

Figure 3 shows a normal incident sound absorption coefficient (α) for CPE/DBS (50:50 w/w) untreated and annealed at 50°C for 2 weeks. A single peak was observed for the untreated sample, and three peaks were observed for the annealed sample. In the annealed sample, a small peak around 300 Hz, a large peak around 550 Hz, and a broad peak around 1000 Hz were labeled as P_L, P_M, and P_H, respectively. In the absorption measurement of a film sample with the backside air layer, the single apparent sound absorption peak was observed by the resonance of the sample and the backside air layer between the sample and the movable wall, as shown in Figure 2. This sound absorption was not caused by the sample itself. A peak frequency of the apparent sound absorption (f_{res}) was estimated by the following equation:

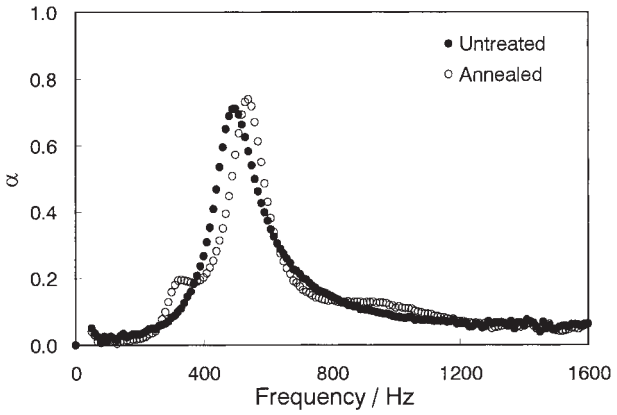

Figure 3 Sound absorption coefficient (α) for CPE/DBS (50 : 50 w/w) untreated and annealed at 50°C for 2 weeks.

$$f_{res} = \frac{1}{2\pi}\sqrt{\frac{\rho \cdot c^2}{m \cdot h} + \frac{k}{m}} \quad (2)$$

where ρ is the air density, c is the speed of sound, m is the surface density of the sample, h is the thickness of the backside air layer, and k is the bending stiffness of the sample.

The measured frequency of P_M was in good agreement with the frequency calculated by eq. (2) for all the samples. Thus, we did not take the contribution of P_M into consideration in this study. An increase in the frequency of P_M for the annealed sample was caused by an increase in the bending stiffness of the sample. There was no sound absorption by the sample itself because the observed absorption peak corresponded to P_M in the untreated sample. On the other hand, two sound absorption peaks, P_L and P_H, were clearly observed for annealed samples. We found the annealed CPE/DBS showed new sound absorption peaks. Evidently these peaks were related to a fine-structure change by annealing treatment.

Figure 4 shows the DSC curves for the same samples as used in Figure 3. We observed a broad exo-

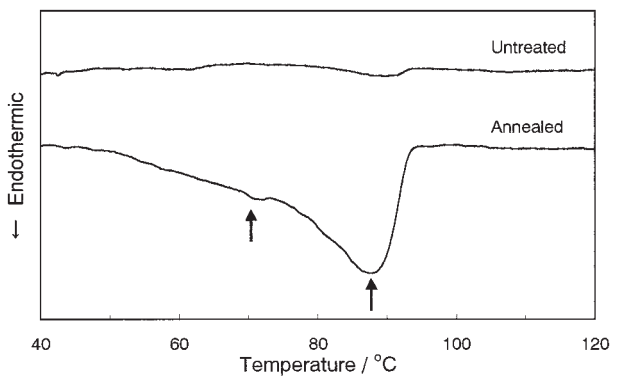

Figure 4 DSC curves for CPE/DBS (50 : 50 w/w) untreated and annealed at 50°C for 2 weeks.

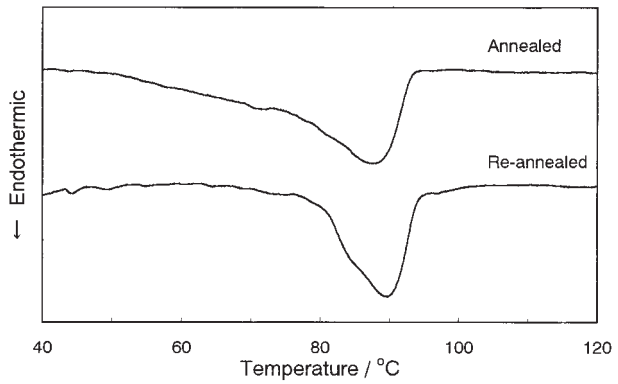

Figure 5 DSC curves for CPE/DBS (50:50 w/w) annealed at 50°C for 2 weeks and reannealed at 85°C for 1 week.

thermic peak around 70°C and a small endothermic peak around 90°C for the untreated sample. Because of the two peaks were almost equal in area, the untreated sample was amorphous by quenching just after the melt-pressing. In the annealed samples we observed two endothermic peaks of melting of crystals. One was the main peak, around 88°C, and the other was the broad peak, around 70°C, shown as a shoulder in the curve of the annealed sample. The two kinds of DBS crystals with different thermal stabilities were considered to have been formed by annealing treatment because CPE is totally amorphous and DBS is essentially a crystalline compound. We designated the crystal with the lower melting point as crystal-L and that with the higher melting point as crystal-H. The melting point of each kind of crystal grown in the CPE matrix was lower than that of the neat DBS crystal. The thermal stability of a crystal is dominated by its size and how perfect it is. Therefore, the DBS crystals grown in the polymer matrix were smaller and/or more disordered than the neat DBS crystals. This was because a polymer matrix disturbs crystallization of DBS molecules. Likewise, crystal-L was smaller and/or more disordered than crystal-H.

To elucidate the cause of the sound absorption observed in Figure 3, we modified the fine structure of the system by a reannealing treatment—annealing again at an arbitrary temperature. Figure 5 shows the DSC curve of the sample reannealed at 85°C, which is between the melting points of crystal-L and crystal-H, for 1 week after being annealed at 50°C for 2 weeks. The DSC curve for the sample annealed at 50°C for 2 weeks also is shown for comparison. The area of the melting peak of crystal-L was diminished notably by the reannealing treatment. A part of crystal-H also was melted because the sample was reannealed at 85°C, which is near the melting point of crystal-H and high enough to melt crystal-L fully.

Figure 6 shows a normal incident sound absorption coefficient for the same sample shown in Figure 5. Though the sound absorption peaks P_L and P_H were observed in the annealed samples, the corresponding peaks were not observed in the reannealed samples, which had no crystal-L. We found that, as a result, the crystal-L contributed to the two sound absorption peaks, P_L and P_H.

Both crystal-L and crystal-H are composed of DBS molecules, but they had different effects on sound absorption. Thus, the sound absorption was greatly influenced by the morphology of these crystals. We conducted WAXD measurement to elucidate the effect of the crystals. We believe there were two types of factors sensitive to the intensity profile by the reannealing treatment: a decrease in specific diffraction intensity and a sharpening of diffraction peaks. For the former, if the two kinds of crystals, crystal-L and crystal-H, belonged to different crystal systems, the intensity profile of the annealed sample would be the superposition of diffraction peaks corresponding to each crystal. Then, the diffraction peaks corresponding to crystal-L would decrease, as the weight fraction of crystal-L decreased by the reannealing treatment.

For the other factor, the sharpening of diffraction peaks, if the two kinds of crystals belonged to the same crystal system, that is, each crystal type was different in size and/or perfection, producing a difference in the melting point, crystal-L would be smaller and/or more disordered than crystal-H. The half-value width of the diffraction peaks would become broader as the crystal size became smaller, with this relationship represented by the Scherrer formula. Also, the half-value width would become broader with decreasing perfection because a disordered crystal is considered to have a mosaic structure assembled of slightly disoriented small crystals.[14] Accordingly, a decrease in crystal-L by the reannealing treatment would diminish half-value width of the diffraction peaks.

Figure 7 shows the WAXD intensity profiles of the same samples as those shown in Figure 5. We did not

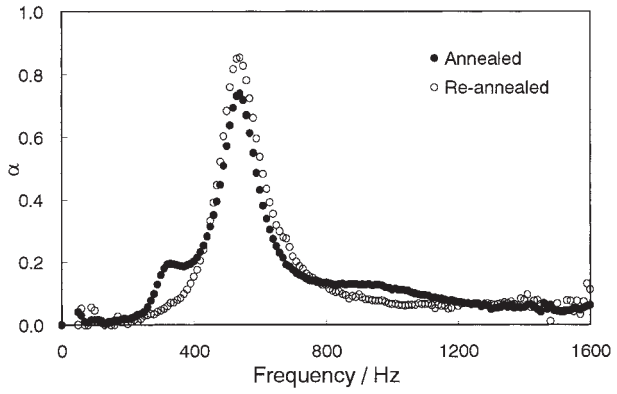

Figure 6 Sound absorption coefficient (α) for CPE/DBS (50 : 50 w/w) annealed at 50°C for 2 weeks and reannealed at 85°C for 1 week.

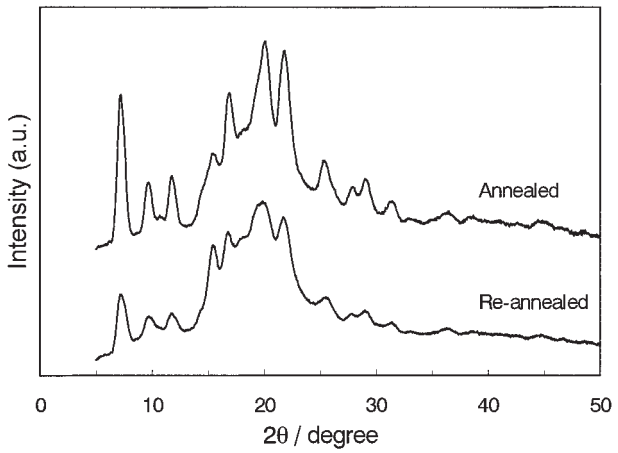

Figure 7 Wide-angle X-ray intensity profiles for CPE/DBS (50 : 50 w/w) annealed at 50°C for 2 weeks and reannealed at 85°C for 1 week.

observe a specific peak intensity that was eliminated or disappeared in the reannealed samples.

Furthermore, we conducted the peak resolution, using the Gauss function as the diffraction peaks corresponding to the DBS crystals, and the intensity profiles of each amorphous profile of CPE and DBS. The positions of separated peaks for annealed and reannealed sample corresponded to those for neat DBS crystal. Figure 8 shows a comparison of the peak position [Fig. 8(a)] and half-value width [Fig. 8(b)] of each peak of the annealed sample ($2\ \theta_{an}$, $\Delta 2\ \theta_{an}$) with that of the reannealed sample ($2\ \theta_{re}$, $\Delta 2\ \theta_{re}$). Evidently, no peak showed changes in the peak position and half-value width from reannealing treatment. The results from WAXD measurement did not agree with the two assumptions mentioned above. It was evident that crystals with sufficient size and perfection were essential for X-ray diffraction. Although the crystal-H was of sufficient size and perfection to be measured in WAXD, the crystal-L was too small and/or disordered to carry out X-ray diffraction. Another possibility is that the half-value width of peaks corresponding to crystal-L was so wide that the diffraction peaks corresponding to crystal-L were smeared in amorphous profiles because the crystal-L was small and/or disordered. To investigate the fraction of each kind of crystals, we calculated it from the crystallinity obtained from both DSC and WAXD measurement. DSC was able to measure the crystallinity of all crystals including small and/or disordered ones, whereas WAXD was able to measure only the crystallinity of crystals of sufficient size and perfection. Hence, crystallinity from WAXD measurement corresponds to the fraction of crystal-H (χ_H), and the difference between the crystallinity from DSC and that from WAXD measurement corresponds to that of crystal-L (χ_L).

Table I shows the χ_L and χ_H of samples annealed at 50°C for 2 weeks and reannealed at 65°C, 75°C, and 85°C for 1 week. The fraction of crystal-L almost disappeared by the reannealing treatment at 85°C and that of crystal-H decreased to some extent. These results are in agreement with the change in the behavior obtained from DSC curves and WAXD intensity profiles. Therefore, the calculation of the fraction of each kind of crystals seems to be reasonable. As the rean-

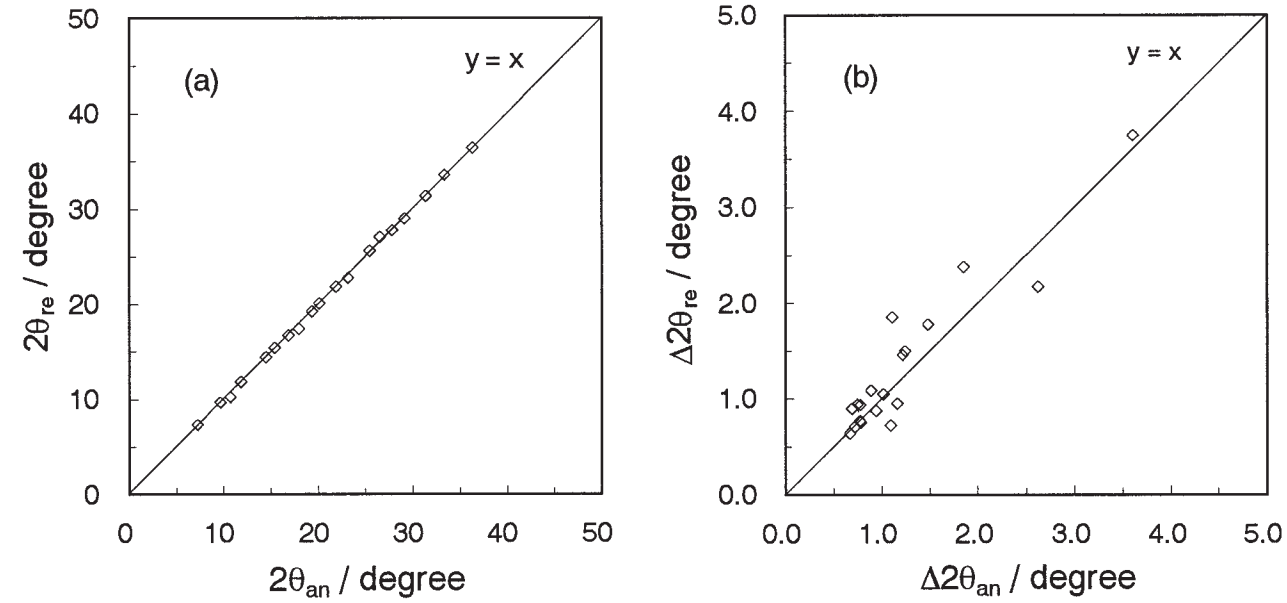

Figure 8 (a) Peak position and (b) half-value width comparison of each peak of CPE/DBS (50 : 50 w/w) annealed at 50°C for 2 weeks and reannealed at 85°C for 1 week, obtained by the curve resolution of wide-angle X-ray intensity profiles in Figure 7.

TABLE I
Crystallinity from WAXD (χ_H) and Difference between Crystallinity from DSC and WAXD (χ_L) for CPE/DBS (50 : 50 w/w) annealed at 50°C for 2 Weeks and Reannealed at Each Temperature for 1 Week

Sample	χ_L (%)	χ_H (%)
Annealed at 50°C	9.6	31.3
Reannealed at 65°C	7.2	30.9
Reannealed at 75°C	1.8	26.0
Reannealed at 85°C	0.7	22.9

TABLE II
Crystallinity from WAXD (χ_H) and Difference between Crystallinity from DSC and WAXD (χ_L) for CPE/DBS (50 : 50 w/w) Annealed at Each Temperature

Annealing temperature (°C)	χ_L (%)	χ_H (%)	Annealing time (week)
30	15.2	31.1	7
40	9.9	32.6	5
50	9.6	31.3	2
65	8.3	27.9	2
75	3.6	25.7	1

nealing temperatures rise, the fraction of crystal-L decreases.

Table II shows the χ_L and χ_H of samples annealed at various temperatures. Samples were annealed for a sufficient time in order to avoid the influence of annealing temperature on the speed of crystallization. Annealing conditions are shown in Table II. Annealing time, in particular, was determined by a time when the crystallinity and the sound absorption reached a constant level, as shown in Table II. As the annealing temperature rose, the fraction of crystal-L decreased. For the annealing treatment at a temperature lower than 50°C, we observed few changes in the fraction of crystal-H, only in about 30%. However, at annealing temperatures higher than 50°C, the fraction of crystal-H decreased because of partial melting of the crystal-H.

Figure 9 shows the dependence of frequency [Fig. 9(a)] and area [Fig. 9(b)] of P_L in normal incident sound absorption coefficient measurement on χ_L for annealed samples and for reannealed samples in various conditions. Regardless of heat treatment such as annealing and reannealing, development of the fractions of crystal-L accompanied the increase in peak frequency and the area of P_L. As a result, it was found that the fraction of crystal-L depended on the annealing or reannealing temperature, and the sound absorption frequency was characterized by the fraction of crystal-L. We were able to specify the sound absorption frequency by optimizing thermal treatment.

CONCLUSIONS

The sound absorption characteristics of CPE/DBS (50 : 50 w/w) as an organic hybrid material were investigated. We newly found two sound absorption peaks around 300 and 1000 Hz by annealing at 50°C for 2 weeks. There were two kinds of DBS crystals

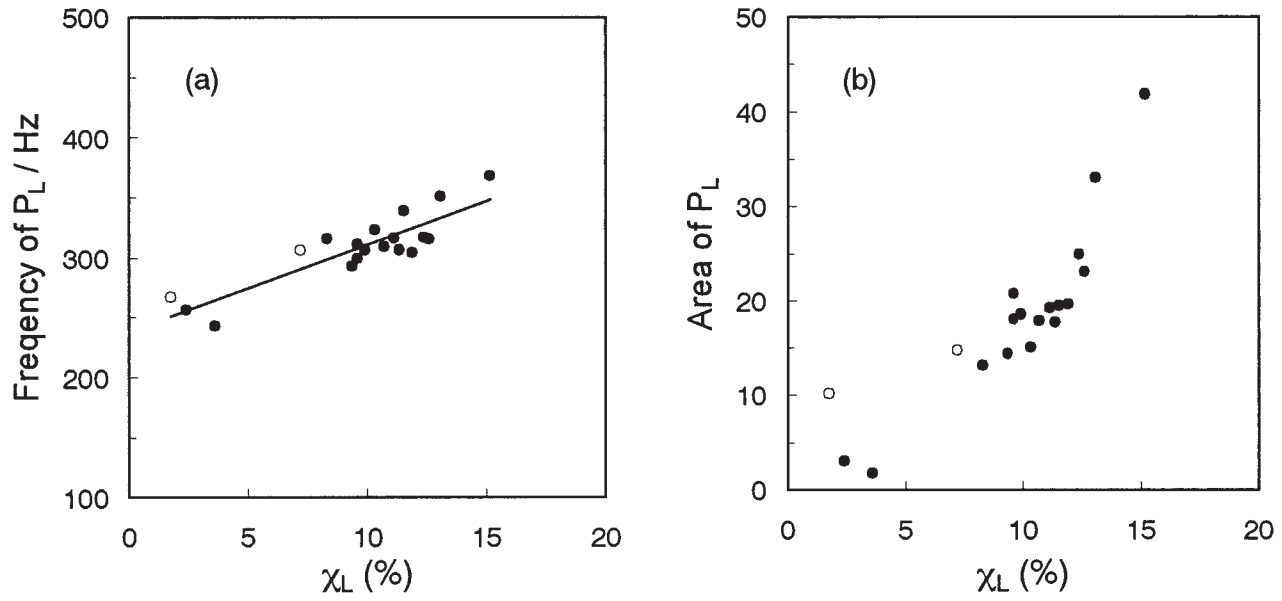

Figure 9 Dependence of frequency and area of P_L obtained from sound absorption coefficient measurement on the difference between crystallinity from DSC and WAXD (χ_L) for CPE/DBS (50 : 50 w/w) annealed and reannealed at various temperatures. Solid circles correspond to annealed samples and open circles to reannealed samples.

with different melting point in the annealed sample. We found the crystal with the lower melting point generated two new sound absorption peaks because the reannealed sample, which only had the crystal with the higher melting point, showed no sound absorption peak. We estimated the fraction of the crystal with the lower melting point from the crystallinity obtained from both DSC and WAXD, where crystal that was small and/or disordered was not related to X-ray diffraction. The fraction of this kind of crystal decreased with increasing temperature of annealing and reannealing. As the fraction of this kind of crystal increased, the frequency and area of sound absorption peak at the lower frequency increased. We found that sound absorption was influenced by the heat treatment such as annealing and reannealing. This is because sound absorption of an annealed organic hybrid material is related to the crystal whose morphology was composed of a filled low-molecular-weight compound.

Annealed CPE/DBS is expected to be applied to a new sound absorber that will have advantages in the thickness of the composing element and in sound absorption characteristics effective in the low-frequency range, in particular. In addition, we have been able to control sound absorption frequency by heat treatment of materials, independent of thickness. This type of sound absorber might be useful as a thin sound absorber component for low frequency because the existing sound absorber requires excessive thickness to absorb the equivalent low-frequency sounds.

References

1. Inoue, K.; Itou, T.; Matsuzaki, I.; Kaneko, H.; Kuromoto, M.; Sumita, M. Sen-i Gakkaishi 2000, 56, 443.
2. Wu, C.; Yamagishi, T.; Nakamoto, Y.; Ishida, S.; Nitta, K.; Kubota, S. J Polym Sci, Part B: Polym Phys 2000, 38, 1341.
3. Wu, C.; Yamagishi, T.; Nakamoto, Y.; Ishida, S.; Nitta, K.; Kubota, S. J Polym Sci, Part B: Polym Phys 2000, 38, 2285.
4. Wu, C.; Yamagishi, T.; Nakamoto, Y.; Ishida, S.; Kubota, S.; Nitta, K. J Polym Sci, Part B: Polym Phys 2000, 38, 1496.
5. Wu, C.; Yamagishi, T.; Nakamoto, Y.; Ishida, S.; Nitta, K. J Polym Sci, Part B: Polym Phys 2000, 38, 2943.
6. Wu, C. J Polym Sci, Part B: Polym Phys 2001, 39, 23.
7. Inoue, K.; Ito, T.; Miura, T.; Wu, G.; Kuromoto, M.; Sumita, M. Sen-i Gakkaishi 2001, 57, 47.
8. Wu, C.; Akiyama, S. J Polym Sci, Part B: Polym Phys 2004, 42, 209.
9. Wu, C. J Mater Sci 2004, 39, 1249.
10. Wu, C. Chinese J Polym Sci 2001, 19, 455.
11. Imai, Y.; ASANO, T. J Appl Polym Sci 1982, 27, 183.
12. Kitamura, M. J Cryst Growth 2002, 237–239, 2205.
13. Kitamura, M.; Furukawa, H.; Asaeda, M. J Cryst Growth 1994, 141, 193.
14. Cullity, B. D. Elements of X-Ray Diffraction; Addison-Wesley: Boston, 1956; Chapter 3.